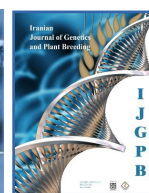**IJGPB**
Iranian Journal of Genetics and Plant Breeding
Print ISSN : 2251-9610
Online ISSN : 2676-346X

Antibacterial and antifungal activity of green synthesized silver nanoparticles using aqueous extracts of *Silybum marianum* L. and *Portulaca oleracea* L.

Saeid Nasirvand[1], Rasool Asghari Zakaria[1*], Hossein Ali Ebrahimi[2]

[1]*Department of Crop Production and Genetics, Faculty of Agriculture, University of Mohaghegh Ardabili, Ardabil, Iran.*
[2]*Department of Pharmaceutics, School of Pharmacy, Ardabil University of Medical Sciences, Ardabil, Iran.*
Corresponding author, 0000-0002-1613-4455. Email: r-asghari@uma.ac.ir.

ABSTRACT INFO

Research Paper

ABSTRACT

The use of plant extracts to produce metal particles at the nanoscale has attracted intensive research interest due to their cost-effectiveness and eco-friendliness. This study aimed to investigate the synthesis of silver nanoparticles (AgNPs) using aqueous extracts of *Silybum marianum* L. and *Portulaca oleracea* L. and to assess their effectiveness as antibacterial and antifungal agents using the agar-well diffusion method. The production of AgNPs was confirmed through spectrophotometry, and their size and shape were measured using Transmission Electron Microscopy (TEM). The role of organic compounds in nanoparticle synthesis was also explored through Fourier Transform Infrared Spectroscopy (FTIR). The FTIR analysis identified the functional groups of organic compounds in *S. marianum* and *P. oleracea* extracts that were responsible for reducing Ag ions and capping the resulting AgNPs. The nanoparticles demonstrated potent antimicrobial properties against *Escherichia coli*, *Staphylococcus aureus*, *Fusarium graminearum*, and *Alternaria alternata*. It was concluded that, in addition to their unique medicinal properties, *S. marianum* and *P. oleracea* can be utilized in the production of AgNP for medical and pharmaceutical purposes against Gram-positive and Gram-negative bacteria, as well as fungal infections. In summary, the seed extracts of *S. marianum* and *P. oleracea*, which are among the available plant sources, can be used for the highly stable production of AgNPs as a reducing and capping agent.

Key words: Antibacterial activity, Green synthesis, *Portulaca oleracea,* Silver nanoparticles*, Silybum marianum.*

INTRODUCTION

Nanoparticles are involved in wide applications used in pharmacy, drug design, and biology (Tan *et al.*, 2006). Various physical and chemical methods have been developed for nanoparticle synthesis, including lithography, chemical reduction, electrochemistry, lasers, and microwaves (Sharma *et al.*, 2019). Of all metallic nanoparticles, silver nanoparticles have garnered significant attention and are widely utilized as antimicrobial agents for disease treatment and for preserving food and water (Wang *et al.*, 2018). Silver nanoparticles also have antimicrobial, anticancer, and antioxidant properties (Elemike *et al.*, 2018). The bioactivity of silver particles depends on their physical and chemical properties, especially their dimensions. So, their antimicrobial properties are significantly increased by converting to small-sized particles at a nanometer range (Kaviya *et al.*, 2011).

In recent years, many researchers have considered the use of plants as sustainable and accessible sources for the production of biocompatible nanoparticles. This approach has several benefits, including biocompatibility, low cost, lack of toxicity, and the production of high-purity nanoparticles (Sharma *et al.*, 2007). Phytochemicals such as tannins, terpenoids, alkaloids, and flavonoids are abundantly found in medicinal and aromatic plants. This category of plants has attracted attention due to their significant potential benefits for society and humans, particularly in medicine. Today, these natural substances serve as a basis for the production of contemporary medications that are widely used (Dorman *et al.*, 2000).

Milk thistle (*Silybum marianum*) is one of the plants that has been used since ancient times for medicinal and therapeutic purposes due to its high antioxidant properties, and restorative and anti-inflammatory effects. Currently, milk thistle is available in pharmacies to treat hepatitis and fatty liver. The seed extract of this plant has many compounds, such as silybin A and B, silydianin, silycristine, apigenin, dihydrosilibine, etc. The dried seed extract of the plant contains 1 to 4% of silymarin, which includes flavonoids such as silybin A and B, silydianin, silycristine, and dihydrosilibin (Schulz *et al.*, 2001). This plant is used to treat many liver disorders characterized by degenerative necrosis and functional impairment (Liperoti *et al.*, 2017). Other medicinal properties of this plant include lowering blood fat (Škottová *et al.*, 1998), anti-diabetics (Malekinejad *et al.*, 2012), anti-arthritis (Gupta *et al.*, 2000), anti-cancer (Singh *et al.*, 2008), and anti-alzheimer (Duan *et al.*, 2015) effects.

Purslane (*Portulaca oleracea* L.) belonging to the Portulacaceae family, is used as a disinfectant, antioxidant, and anti-hemorrhoid, and has many therapeutic uses in preventing myocardial infarction and strengthening the immune system. This plant is rich in beta-carotene, flavonoid, monoterpene glycoside, alkaloid, antioxidant, and omega-3. The aerial parts of this plant have anti-inflammatory properties equivalent to diclofenac sodium (Iranshahy *et al.*, 2017). This plant possesses several medicinal properties such as analgesic, antibacterial, anti-inflammatory, anticonvulsant, diuretic, antispasmodic, wound-soothing, and skeletal muscle relaxing effects. It is useful in treating various ailments, including respiratory disorders, gastrointestinal diseases, liver inflammation, kidney and bladder ulcers, fever, insomnia, inflammation, and headache (Rahimi *et al.*, 2005).

Fusarium graminearum, the cause of Fusarium Head Blight (FHB) on wheat and barley, is a significant threat to food safety and security. It not only reduces crop yields but also contaminates the grain with trichothecenes, particularly deoxynivalenol (DON), whose consumption can have adverse effects on human and animal health. FHB symptoms, such as bleaching and necrosis, appear three days after infection and affect wheat and barley floral structures (Brown *et al.*, 2010).

Alternaria alternata is a common pathogen in various natural food products, including fruits and vegetables, seeds, and cereals, which produces several mycotoxins such as alternariol, alternariol methyl ether, tenuazonic acid, and altertoxins. Although *A. alternata* is the primary species producing such toxins, other species such as *Alternaria citri*, *Alternaria solani*, *Alternaria longipes*, and *Alternaria tenuissima* may produce similar toxins. The production of *Alternaria* mycotoxins has been reported in a range of infected natural fruits and vegetables, including grapes, tomatoes, lemons, apples, oranges, mandarins, blueberries, and olives (Barkai-Golan *et al.*, 2008).

Silver nanoparticles have shown promising results in inhibiting the growth of various plant pathogens, which has made them a valuable tool in crop protection. With the increasing demand for sustainable agricultural and environmentally friendly practices, the use of silver nanoparticles can be considered as a non-toxic alternative to traditional chemical pesticides. Considering the high potential of silver nanoparticles in combating bacterial and fungal diseases in plants, this study aimed to assess the potential of the *S.*

marianum L. and *P. oleracea* L. seed extracts in the synthesis of silver nanoparticles. Also, the antibacterial and antifungal properties of the biosynthesized nanoparticles against *E. coli* and *S. aureus* bacteria and *F. graminearum* and *A. alternata* were evaluated.

MATERIALS AND METHODS

Preparation of plant extracts
In this study, we used the aqueous extracts of *S. marianum* and *P. oleracea*. For this purpose, the seeds were first washed with sterile distilled water for 15 min and then dried at room temperature. Then, 40 g of powdered seeds were added to 200 mL of distilled water and placed in a shaker at room temperature for 48 h. To remove impurities, the extracts were then centrifuged at 100 rpm for 10 min. The resulting extracts were stored at 4 °C until use (Nikbakht *et al.*, 2015).

Biosynthesis of silver nanoparticles
10 mL of the aqueous extracts of *S. marianum* and *P. oleracea* seeds were added to 90 mL of 1 mM silver nitrate to reduce silver ions. The solution was placed on a shaker for 72 h at room temperature and in the dark according to Jacob *et al.* (2012). The change in the color of the extract solution from light yellow to dark brown or black implies the synthesis of silver nanoparticles (Dousti *et al.*, 2019). In the next step, the solution was centrifuged for 15 minutes at 15,000 rpm, and after discarding the supernatant, the residue was washed with water and alcohol and dried with a freeze-dryer. The obtained silver nanoparticles were kept at 4 °C for further study (Ajitha *et al.*, 2015; Devanesan *et al.*, 2021).

Transmission electron microscopy (TEM)
Transmission electron microscopy (TEM, EM10C-100Kv model, Zeiss, Germany) was used to investigate the morphology of synthesized silver nanoparticles. For this purpose, the nanoparticle sediments were centrifuged three times at 12,000 rpm, and the resultants were photographed by electron microscopy. In this way, the nanoparticles were fixed on a copper mesh covered with carbon, and after drying with an infrared lamp, photography was performed with an accuracy of 2.32 A° (Mishra *et al.*, 2014).

Infrared assay of silver nanoparticles
The interaction or bonding of nanoparticles in the reaction mixture as well as the determination of plant factors in the reduction of silver ions were investigated using a Fourier Transform Infrared Spectrometer (FTIR spectroscopy, RX1 model, Perkin Elmer,

United Kingdom) with the range of 400–4000 cm^{-1}. Infrared detection was performed to identify different functional groups and biomolecules responsible for reducing silver ions (Kalaiarasi *et al.*, 2013).

XRD analysis
The dried AgNPs sample was targeted by X-ray diffraction XRD, MPD 3000 model, Company construction of Ital structure, Italy) for structural crystallography. After sample preparation, the crystalline nature of AgNPs was confirmed by the XRD pattern obtained from MPD 3000 X-ray diffractometer at 2θ range from 0 to 100°. The pattern was recorded by CuKα radiation with λ of 1.5406 A° at a voltage of 40 kV and a current of 15 mA with a scan rate of 10° min^{-1} (Ahmad *et al.*, 2010; Okafor *et al.*, 2013).

Antibacterial Activity
Agar-well diffusion method with minor modification was used to determine the antimicrobial activity of prepared nanoparticles. First, according to the McFarland standard, the *S. aureus* and *E. coli* bacteria were completely spread by cell spreader on Petri dishes containing solid LB medium. Then wells with the same diameter were created in the culture medium, and different concentrations (25, 100, and 200 μg mL^{-1}) of nanoparticles were added to each of the wells. The plates were then placed in an incubator at 37 °C and left for 24 h. The diameter of the bacteria's growth-inhibited area was determined using Image J software and compared with the control group (Fatima *et al.*, 2015; Ahmed *et al.*, 2017).

Determination of the minimum inhibitory concentration (MIC) and minimum bactericidal concentration (MBC)
The effect of different concentrations of synthesized AgNPs on the growth of bacteria was investigated using 96-well microplates. Initially, 95 μL of Muller-Hinton medium was added to each well of the 96-well microplates. Subsequently, 100 μL of AgNPs at a concentration of 100 μg mL^{-1} was added to the first well. The nanoparticles were then diluted by half in each subsequent well, creating a dilution series until the last well, where the concentration of nanoparticles was half that of the previous well. The last well, serving as the negative control, contained 195 μL of Hinton Broth molar and 5 μL of microbial suspension but lacked the test compound. All wells, except the first one, were inoculated with 5 μL of bacterial suspension equivalent to 1.5×108 CFU mL^{-1}. The turbidity of the wells was observed, and bacterial growth or lack thereof was examined. To determine the Minimum Bactericidal Concentration (MBC) of nanoparticles, the wells with

inhibited growth were cultured with a sterile loop on Muller-Hinton medium and then incubated at 37 °C for 24 h. The lowest concentration of nanoparticles at which no bacteria appeared was considered the MBC. Throughout the study, the effect of the synthesized nanoparticles on the standard sample was repeated three times, with two controls considered for each dilution series (Maiti *et al.*, 2014; Singh *et al.*, 2020; Al-Enazi *et al.*, 2023).

Antifungal activity of AgNPs
The antifungal activity of AgNPs was evaluated through monitoring the inhibition of mycelium expansion. Three concentrations of NPs i.e. 25, 100, and 200 μg mL^{-1} were prepared in a Potato Dextrose Agar (PDA) medium by autoclaving. Fresh cultures of *F. graminearum* and *A. alternata* were used to create 6-mm agar plugs, which were then transferred to the medium containing varying concentrations of synthesized AgNPs. Control plates did not contain AgNPs. Following incubation at 28 °C, the average radius of fungal growth was measured. The growth inhibition of mycelium was evaluated using the formula: Mycelium growth percentage=(R-r)/R×100, where R is the mean radius of the control and r is the radius of samples treated with nanoparticles. Data were processed using SAS statistical analysis with the Duncan test. (Kim *et al.*, 2012; Fouda *et al.*, 2023). All

treatments were conducted in triplicates.

RESULTS

Green synthesis of AgNPs
In this study, the green synthesis of AgNPs was conducted using *S. marianum* and *P. oleracea* extracts to reduce silver ions. The initial sign of silver nanoparticle production is a change in solution color, from yellow to brown, upon the addition of plant extracts to the silver nitrate solution. The color then darkened to a deep brown after 12 h in *P. oleracea* and 24 h in *S. marianum*, indicating the production of nanoparticles. The color change of the reaction mixture is the primary indicator of the formation of silver nanoparticles, with variations in the amount and intensity of color change between plant extracts. This variation may be due to changes in the quantity of NPs produced or the availability of H$^+$ ions which contribute to the reduction of silver. Figures 1 and 2 show the results of ultraviolet-visible spectroscopy on the *S. marianum* and *P. oleracea* extracts after the synthesis of silver nanoparticles. A visible peak at 400 to 450 nm confirms the presence of silver nanoparticles, which is attributed to the surface plasmon resonance caused by the introduction of free electrons in the nanoparticles (Poulose *et al.*, 2014).
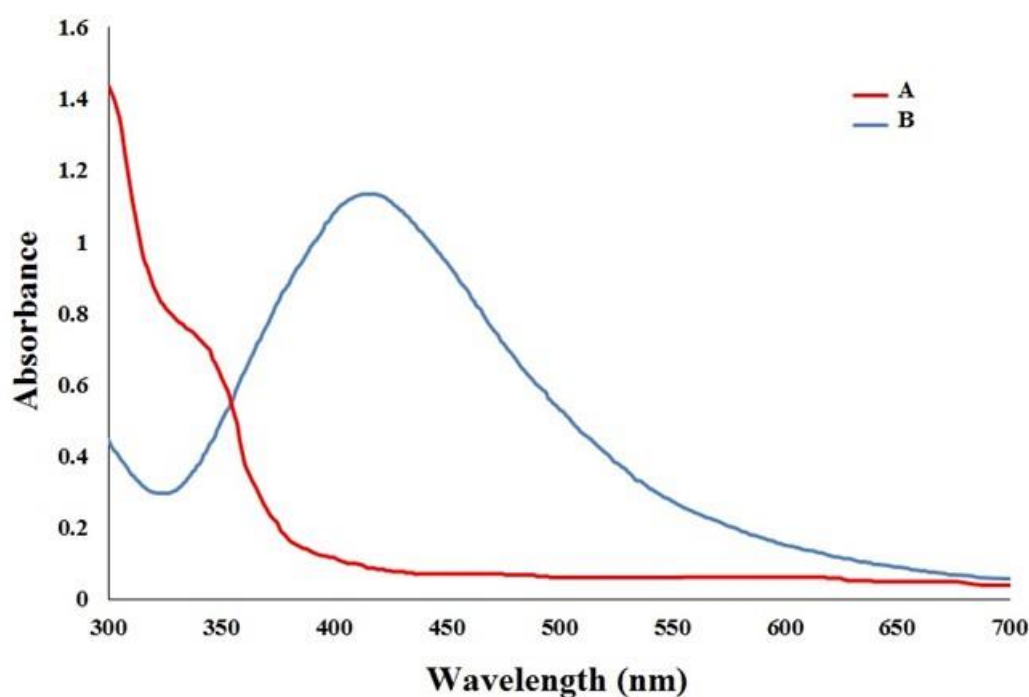

Figure 1. A: UV-Vis absorption spectrum of *S. marianum* seed extract and **B:** silver nanoparticles biosynthesized from *S. marianum* seed extract. According to the graph, the maximum UV absorption of silver nanoparticles was at the wavelength of 410 to 430 nm.
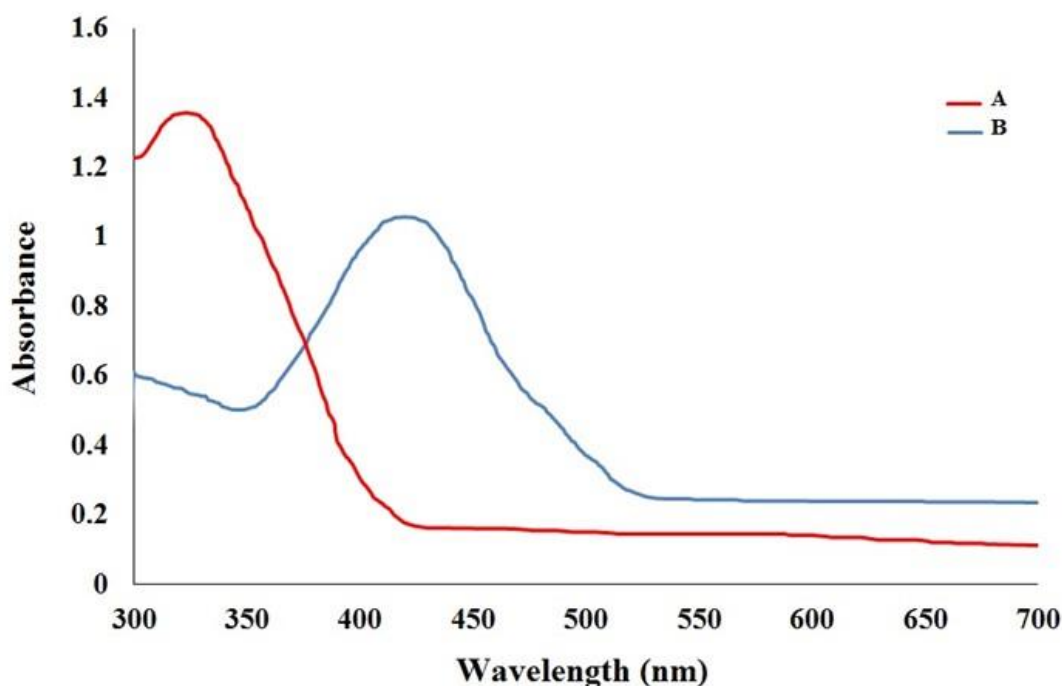
Figure 2. A: UV-Vis absorption spectrum of *P. oleracea* seed extract and **B:** silver nanoparticles biosynthesized from *P. oleracea* seed extract. According to the graph, the maximum UV absorption of silver nanoparticles was at the wavelength of 418 to 422 nm.

FTIR spectroscopy

FTIR analysis (Figure 3) revealed the functional groups of organic compounds in *S. marianum* and *P. oleracea* seed extracts, which are responsible for reducing Ag (I) ions and capping the resulting AgNPs. The absorption peaks identified in the FTIR spectrum of the seed extracts range from 3,200 to 3,600 cm^{-1}, representing the O-H (hydroxyl) and -NH2 (amine) stretching vibrations. The bands at 2924 cm^{-1} and 2925 cm^{-1} arise from C–H stretching in hydrocarbons, ethers, aldehydes, and ketones, as well as O–H stretching in carboxylic acid. The band at 2852 cm^{-1} indicated the C–H stretching in alkanes. Additionally, bands identified at 1630 cm^{-1} and 1654 cm^{-1} come from the N–H bending of amide-II bonds linking amino acids in the protein or –C=C- stretch in alkenes (Sajadi *et al.*, 2016).

Furthermore, a peak at 1,522 cm^{-1} corresponds to the aromatic ring of the terpenoid saponin structure. The C-C stretch in the aromatic ring is identified by the peak found at 1412 cm^{-1}. The peaks in the region 1165 cm^{-1} in nanoparticles are assigned to C-O stretching in alcohols, carboxylic acids, esters, and ethers; C-H waging in alkyl halides and C-N stretching in aliphatic amines. Strong bands in the region 1000–1320 cm^{-1} in both nanoparticles were assigned to C-O stretching in alcohols, carboxylic acids, esters, and ethers. The observations confirmed that the synthesized AgNPs were capped with the secondary metabolites (phenolic and flavonoid compounds) of *S. marianum* and *P. oleracea*. FTIR measurements were carried out to identify the major functional groups in the seed extract and their possible involvement in the synthesis and stabilization of silver nanoparticles (Sivalingam *et al.*, 2023).

X-ray diffraction (XRD)

The addition of 1 mM silver nitrate solution to the seed extract changed its color from yellow to dark brown, indicating the synthesis of AgNPs. After 12 h in *P. oleracea* extract and 24 h in *S. marianum* extract, no significant change in color was observed, and nanoparticle synthesis was deposited after 24 h. The formation of the nano-crystalline Ag particles was further confirmed by the XRD analysis as shown in Figure 4. Bragg reflection of the 2θ peaks was observed at 38.410°, 44.219°, 64.115°, and 77.221°, corresponding to (111), (200), (220), and (311) plane lattice which can be indexed to the face-centered cubic crystal nature of the silver. The broadening of Bragg's peaks in the XRD pattern suggests the formation of nanoparticles (Cullity, 1956). The XRD results showed that the AgNPs produced by *S. marianum* and *P. oleracea* seed extracts have a crystalline structure. Moreover, the absence of additional peaks in the XRD
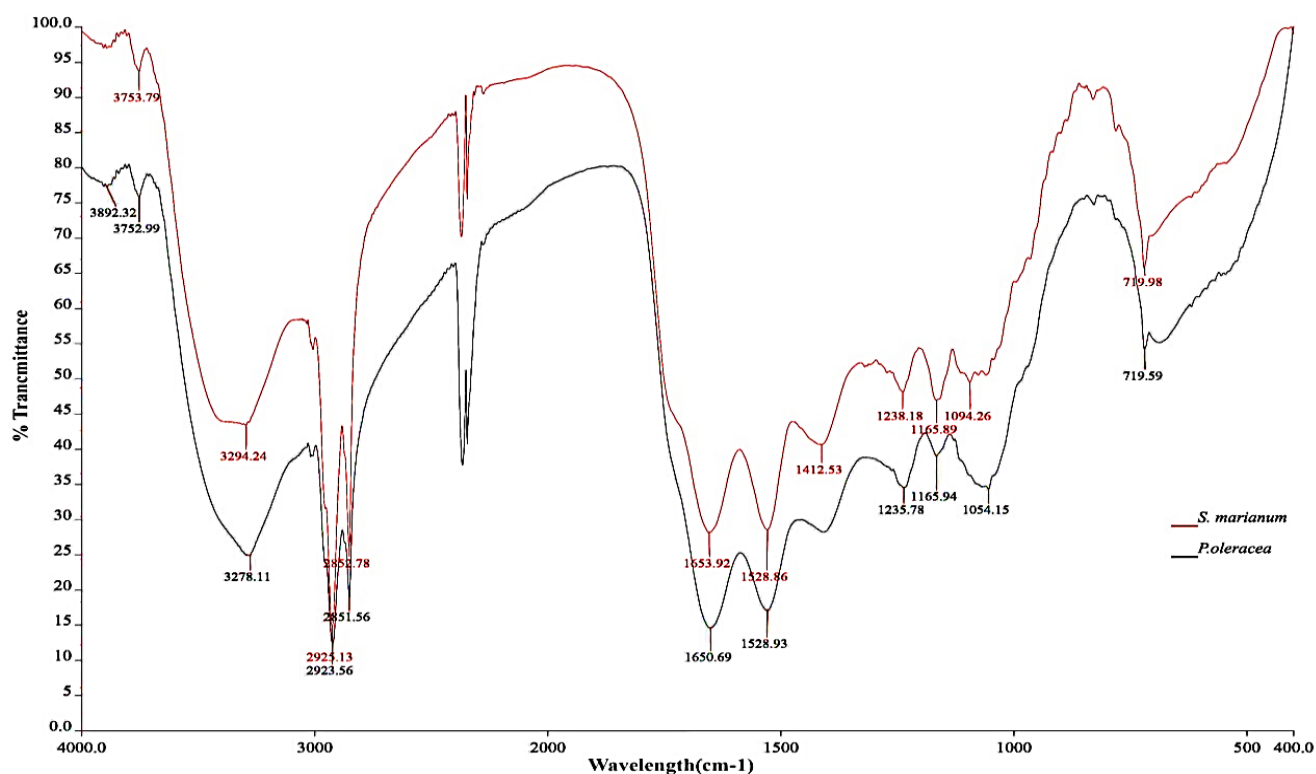
Figure 3. Fourier transform infrared (FTIR) spectrum of *S. marianum* and *P. oleracea* seed-extract-mediated biosynthesized silver nanoparticles and identify active and regenerating groups of silver ions in the range of 400-4000 cm^{-1}.

pattern implies that the biosynthesized AgNPs are highly pure.

Transmission electron microscopy (TEM)
The size and shape of nanoparticles were determined using transmission electron microscopy (TEM). TEM images of the prepared AgNPs and histogram of corresponding particle size distribution from TEM are depicted in Figure 5. These images revealed that the nanoparticles exhibited spherical and oval shapes, with a size between 2 to 50 nm. Some particles appeared elongated due to the aggregation of two or more nanoparticles. The majority of nanoparticles in thistle measured between 20-15 nm (38.69%), while in purslane, the sizes ranged from 20-25 nm (34.34%). It can be inferred that the average size of nanoparticles obtained from purslane extract was larger than that of thistle. Similar findings have been documented for the production of AgNPs, with sizes of 2 to 75 nm, using plant extracts as reducing agents (Chandran *et al.*, 2006; Tripathy *et al.*, 2010; Salari *et al.*, 2019; Pungle *et al.*, 2022). Additionally, the synthesis of silver nanoparticles using *Berberis vulgaris* extract demonstrated particle sizes in the range of 30 to 70 nm (Behravan *et al.*, 2019).

Antibacterial activity of AgNPs
The antibacterial activity of AgNPs was assessed using

Table 1. Analysis of variance for the diameter of inhibition zone of AgNPs synthesized by *S. marianum* and *P. oleracea* on *E. coli* and *S. aureus* bacteria growth.

Source of variation	df	Mean of square	*p*-value
AgNP source (S)	1	3.24	0.0002
AgNP concentration (C)	2	19.9825	0
Bacterial species (B)	1	15.21	0
C×B	2	0.8175	0.0155
C×S	2	0.3225	0.1621
S×B	1	1	0.0211
C×B×S	2	0.0175	0.8993
Error	24	0.1642	
Coefficient of variation (%)		7.97	

the agar-well diffusion method. After 24 h, growth inhibition was observed around the wells loaded with 25, 100, and 200 μg mL^{-1} of AgNPs (Figure 6). The release of inhibitory compounds, such as AgNPs, led to the suppression of bacterial growth around the wells. The analysis of variance (Table 1) revealed that the source and concentration of AgNPs significantly ($p<0.01$) affected the diameter of the growth inhibition zone of bacteria. Additionally, the type of bacteria and its interaction with the AgNPs source or concentration
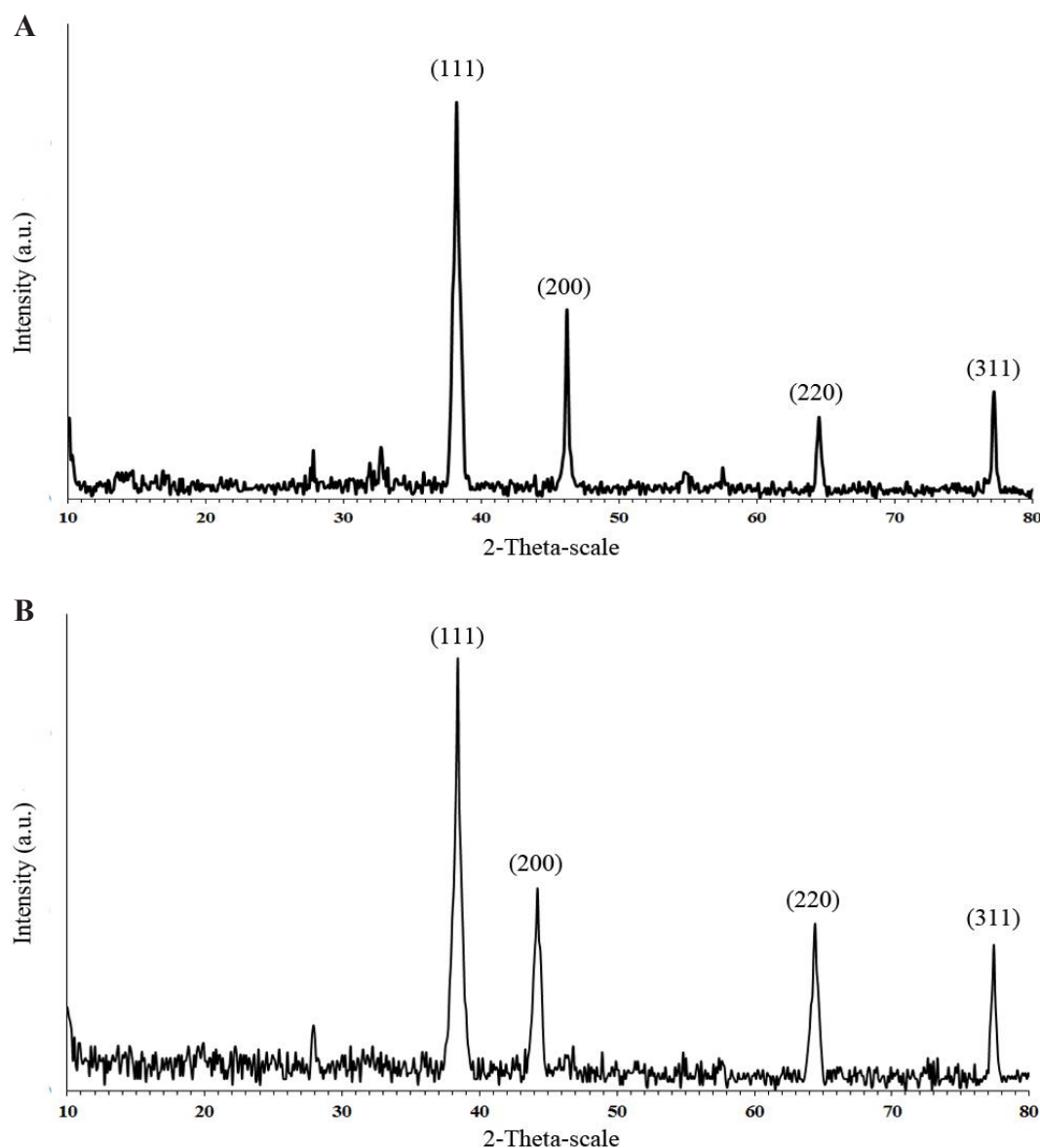
A

B

Figure 4. XRD pattern of silver nanoparticles synthesized by treating AgNO$_3$ solution with **A:** *S. marianum* and **B:** *P. oleracea* seeds extract.

were found to be significant ($p<0.05$). However, the interaction effects of AgNPs source×concentration and AgNPs source×concentration×bacteria type were not significant (Table 1). The results indicated that increasing the concentration of biosynthesized AgNPs in the culture medium resulted in the creation of a larger inhibition zone for both types of bacteria. As shown in Figure 7, Gram-negative bacteria (*E. coli*) exhibited a greater inhibitory region compared to Gram-positive *S. aureus* bacteria at the same concentration of AgNPs. This difference can be attributed to variances in the cell composition of Gram-positive and Gram-negative cells. It is worth noting that AgNPs produced by *S. marianum* and *P. oleracea* demonstrated potent

inhibition against both types of bacteria. The study of antibacterial activity suggested that AgNPs synthesized by both *S. marianum* and *P. oleracea* exhibited strong antibacterial properties against the Gram-negative *E. coli* bacteria with increasing concentrations. However, for Gram-positive *S. aureus* bacteria, the inhibition zone of AgNPs synthesized by *S. marianum* was significantly ($p<0.05$) larger than that of AgNPs synthesized by *P. oleracea* at all studied concentrations (Figure 7).

MIC and MBC generated by AgNPs
The minimum inhibitory concentration and the minimum bactericidal concentration of AgNPs obtained from *S. marianum* and *P. oleracea* extract
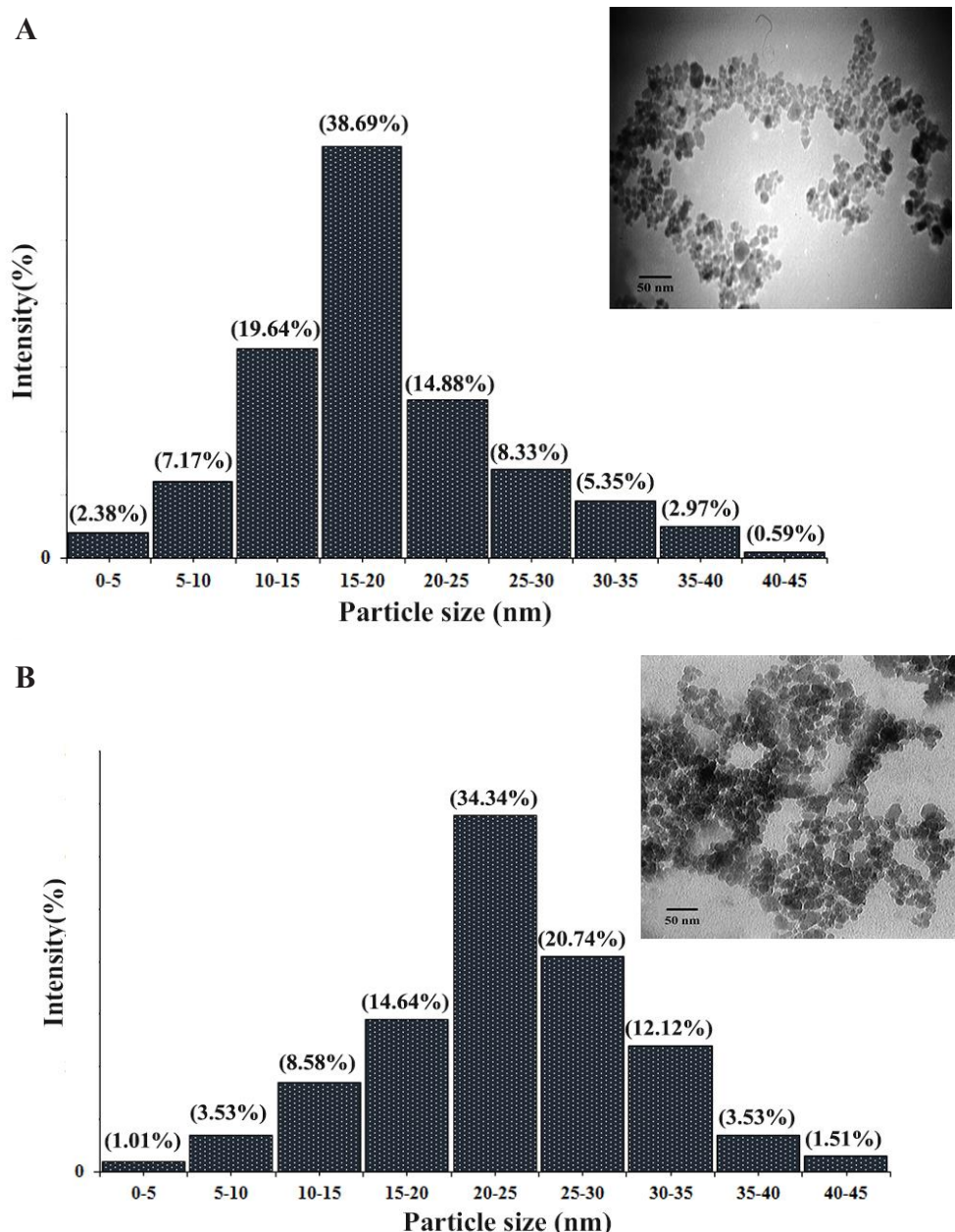
A

B

Figure 5. TEM image and particle size distribution histogram of the biosynthesized AgNPs using **A:** *S. marianum* and **B:** *P. oleracea* seed extracts. The maximum distribution range (38.69%) of nanoparticles was between 15 and 20 nm for *S. marianum* and between 20 and 25 nm (34.34%) for *P. oleracea*.

were determined on *E. coli* and *S. aureus*. As shown in Figure 8, the MIC for AgNPs obtained from *S. marianum*, were 0.78 and 1.56 µg mL^{-1} for *E. coli* and *S. aureus*, respectively. Besides, the MBC were 1.56 µg mL^{-1} and 3.12 µg mL^{-1} for *E. coli* and *S. aureus*, respectively. Also, the MIC values for AgNPs obtained from *P. oleracea*, were 1.56 and 6.25 µg mL^{-1} for *E. coli* and *S. aureus*, respectively, and the MBC values were 3.12 µg mL^{-1} for *E. coli* and 6.25 µg mL^{-1} for *S. aureus*. These results indicated that the MIC and MBC of AgNPs obtained from *S. marianum* on both *E. coli*

and *S. aureus* were lower compared with those from *P. oleracea*.

Antifungal activity of synthesized AgNPs

The synthesized AgNPs exhibited antifungal activity. With an increase in the concentration of biosynthesized AgNPs in the culture medium, the inhibitory effects on mycelium growth in both fungi species increased significantly (Figure 9). Analysis of variance showed that the mycelium growth percentage of both *A. alternata* and *F. graminearum* was significantly
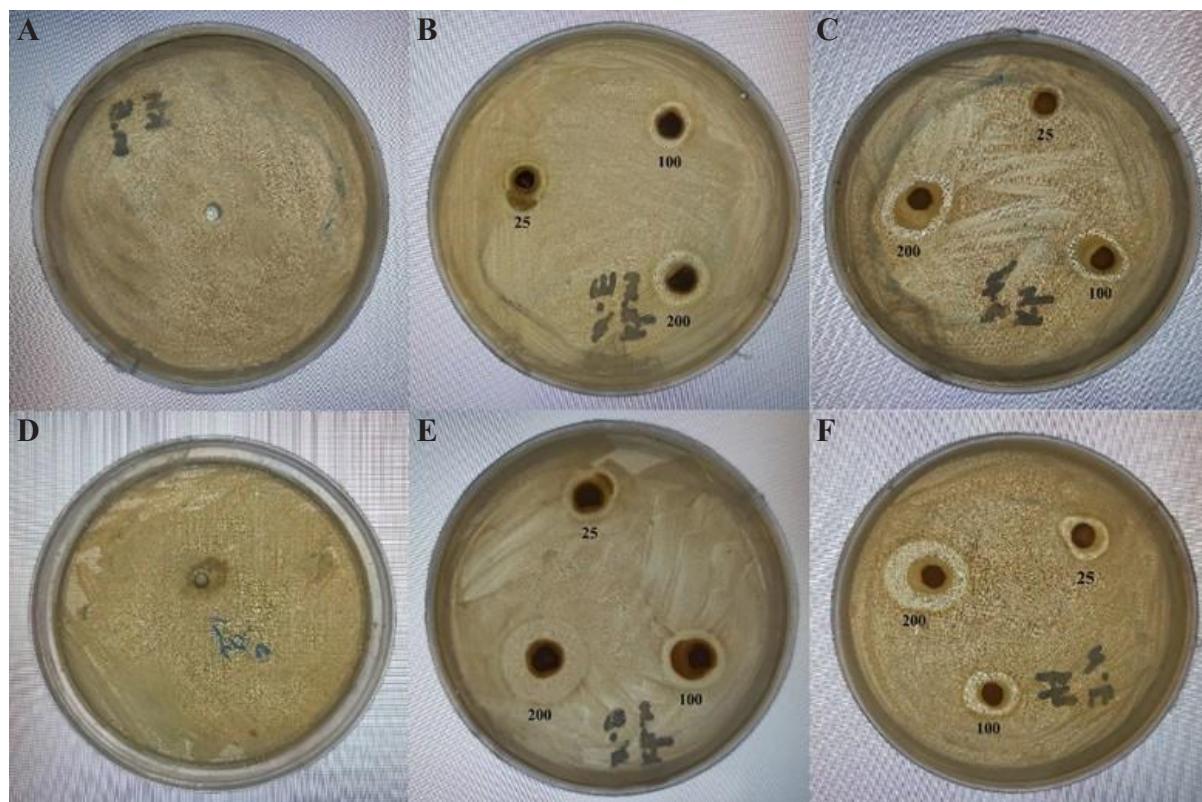
Figure 6. Zone of inhibition of silver nanoparticles synthesized with aqueous extract of *P. oleracea* (**B, E**) and *S. marianum* (**C, F**) against *S. aureus* (**B, C**) and *E. coli* (**E, F**), and control (**A, D**).
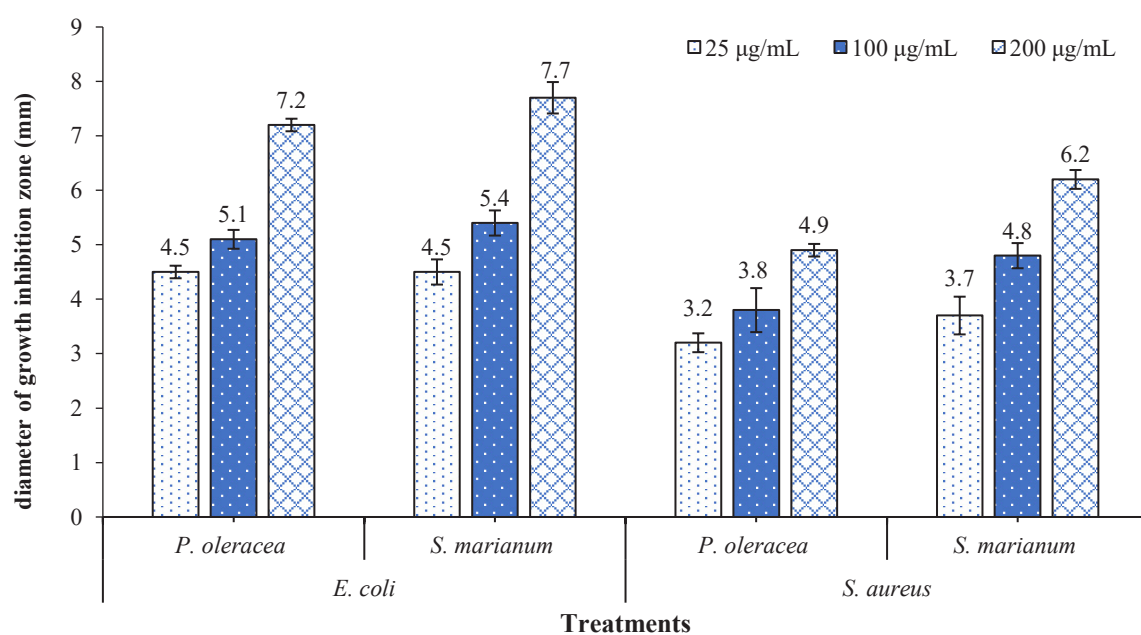

Figure 7. Diameter of growth inhibition zone (mm) of different concentrations of nanoparticles synthesized with aqueous extract of *S. marianum* and *P. oleracea* on *Staphylococcus aureus* and *Escherichia coli*.
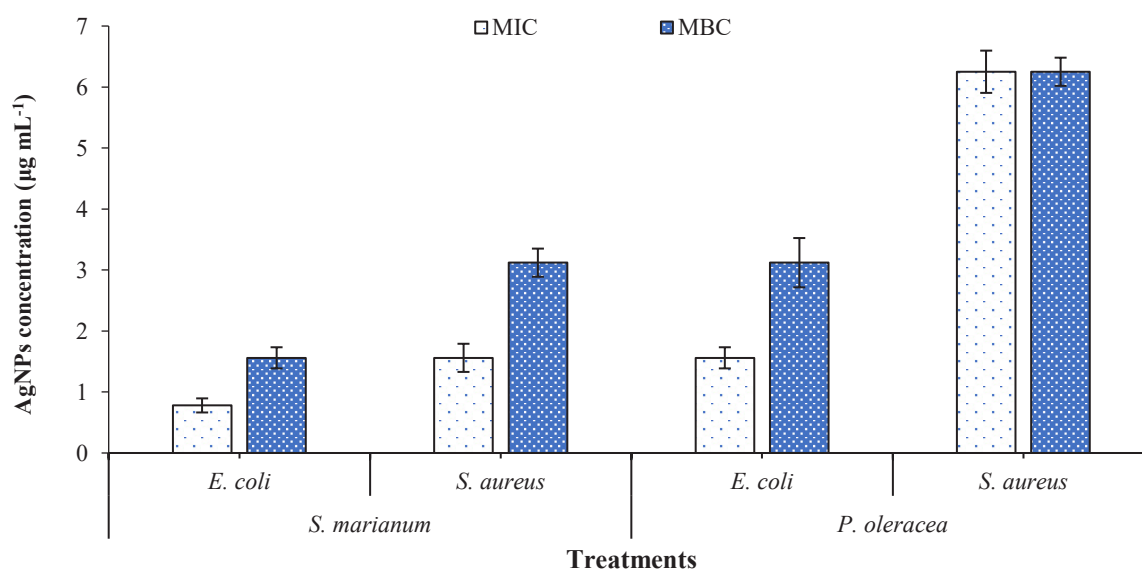
Figure 8. MIC and MBC generated by AgNPs produced by the green method on Gram-positive and Gram-negative bacteria.
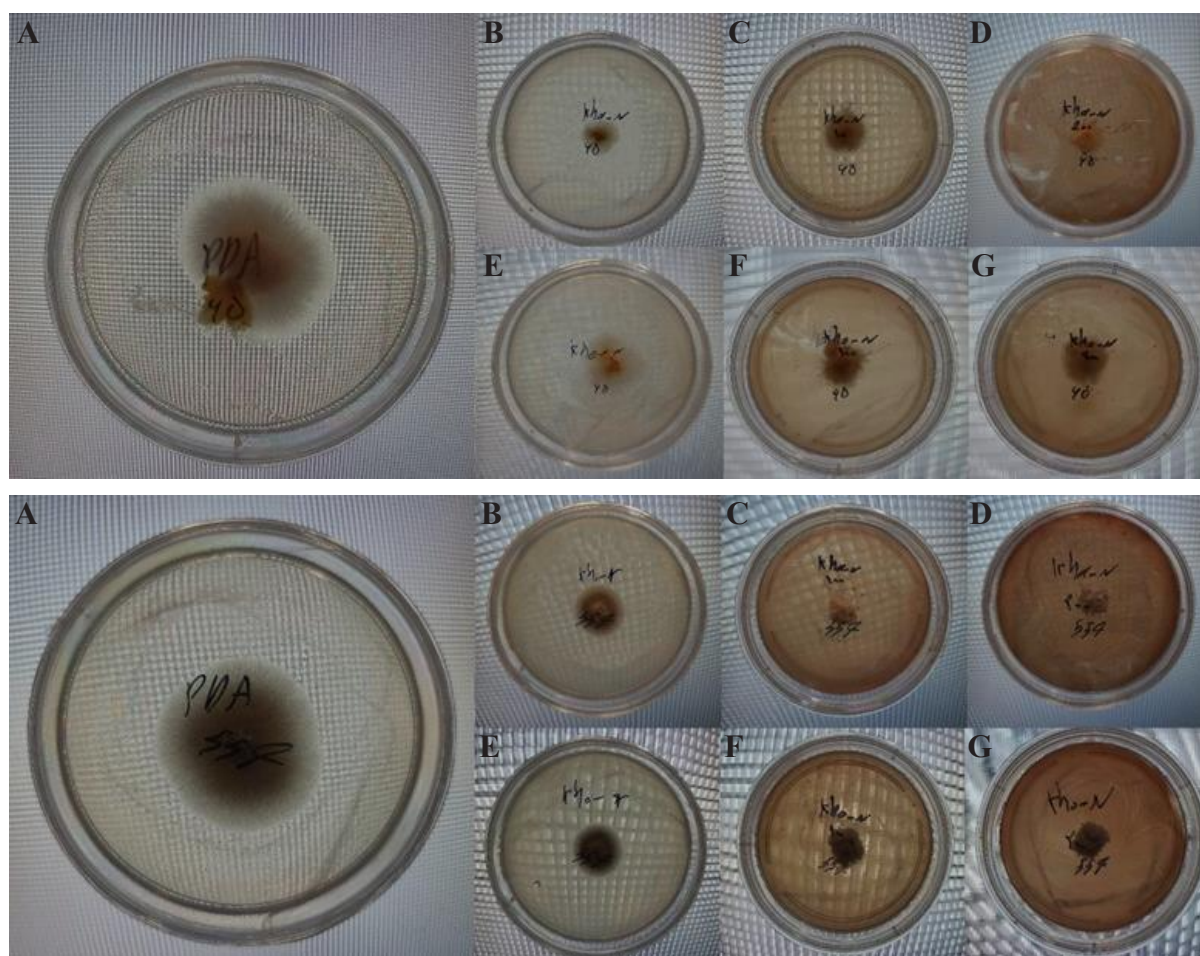
Figure 9. Growth diameter of *F. graminarum* (upper image) and *Alternaria alternata* (lower image) at different concentrations of AgNPs synthesized from *S. marianum* (**B, C, and D**) and *P. oleracea* (**E, F, and G**) in different concentrations of AgNPs: control (**A**), 25 µg mL^{-1} (**B and E**), 100 µg mL^{-1} (**C and F**), and 200 µg mL^{-1} (**D and G**) of AgNPs.

Figure 10. Mycelium growth percentage of *A. alternata* and *F. graminearum* affected by AgNPs synthesized with aqueous extract of *S. marianum* and *P. oleracea*.

($p<0.01$) influenced by the effects due to the source and concentration of AgNPs synthesized with aqueous extract of *S. marianum* and *P. oleracea*, while, other sources of variation showed non-significant differences (Table 2). The highest inhibitory effect was observed in 200 μg mL^{-1} of AgNPs biosynthesized with the aqueous extract of *S. marianum*. For the AgNPs synthesized with the aqueous extract of *P. oleracea*, both concentrations of 100 and 200 μg mL^{-1} similarly showed the greatest inhibitory effect on the mycelium growth of *A. alternata* and *F. graminearum*, while the concentration of 25 μg mL^{-1} significantly showed the lowest inhibitory effect (Figure 10). In addition, the inhibitory effect of AgNPs biosynthesized with an aqueous extract of *S. marianum* on *F. graminearum* was more than that of *A. alternata* (Figure 10). Also, regarding growth morphology, the results showed that at low concentrations of synthesized AgNPs, fungal mycelia were dispersed in the culture medium, while no mycelia dispersion was found with increasing concentration of AgNPs (Figure 9).

DISCUSSION

During the synthesis of AgNPs, Ag$^+$ ions were exposed to the reducing compounds of the extract, initiating the reduction of silver nitrate salt. Silver ions are reduced when exposed to plant extracts in solution and form silver hydrosols. The factor responsible for the Ag$^+$

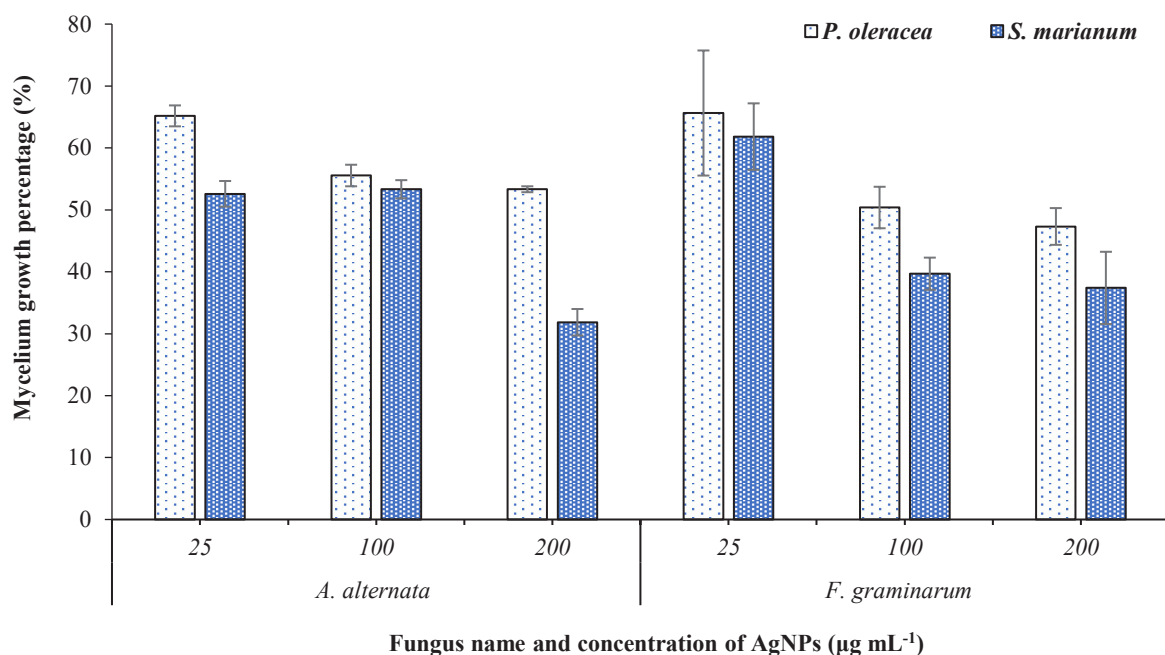**Table 2.** Analysis of variance for the mycelium growth percentage of *A. alternata* and *F. graminearum* affected by AgNPs synthesized with aqueous extract of *S. marianum* and *P. oleracea*.

Source of variation	df	Mean of square	*p*-value
AgNP source (S)	1	921.426	0.0003
AgNP concentration (C)	2	1082.848	0.0000
Fungi species (F)	1	22.8962	0.514
C×S	2	72.3825	0.2691
S×F	1	35.2242	0.4194
C×F	2	156.596	0.0687
S×C×F	2	88.3115	0.2053
Error	24	52.1836	
Coefficient of variation (%)		14.12	0.0003

ions reduction varies depending on the extract type (Jha *et al.*, 2009; Niveditha *et al.*, 2018; Fahes *et al.*, 2023). The color change from light yellow to dark brown resulting from the reaction between the plant extracts and the silver salt solution was consistent with previous studies (Vijayaraghavan *et al.*, 2012; Asghari *et al.*, 2014; Rajoriya *et al.*, 2017; Bhuyar *et al.*, 2020). Silver nanoparticles have a characteristic absorbance peak between 400-450 nm. When the peak exceeds this range, there may be particle aggregation, resulting in the formation of larger particles. Conversely, a peak

shift below this range indicates the presence of other components in the nanoparticle solution. Changes in absorption peak act as a significant indicator of nanoparticle size, quantity, and morphology. Changes in the morphology of synthesized nanoparticles explain the differences in their visual appearance (Chen *et al.*, 2004). Slight changes in the absorption peaks of AgNPs, without significant color alteration, indicate their stability and long-term endurance (Vickers, 2017). The findings of this study regarding the peak of silver nanoparticles at the wavelength of 410-430 were consistent with the results of research conducted by other scholars (Firdhouse *et al.*, 2012; Dousti *et al.*, 2019b).

FTIR analysis revealed that the molecules linked to silver nanoparticles are composed of aromatic rings and amide polyphenols (Kumar *et al.*, 2010; Flieger *et al.*, 2021). Phytochemical screening using FTIR spectroscopy indicated a marked distinction in the composition of bioactive compounds (aliphatic and aromatic) in AgNPs preparation, which potentially serve as crucial factors to explain the mechanism of antifungal activities (Afify *et al.*, 2017). Proteins can create a coating that envelops metal nanoparticles, thus preventing their aggregation and enhancing environmental stability (Basavaraja *et al.*, 2008). Biomolecules are deemed environmentally friendly due to their role in reducing and stabilizing biosynthesized nanoparticles (Huang *et al.*, 2004). Changes in spectrum peaks were observed, while some of them remained unaltered, which means that the proteins may be attached to the AgNPs. It is likely that proteins form a protective covering around the NPs to hinder particle aggregation and sustain their stability in the medium (Basavaraja *et al.*, 2008; Farshbaf *et al.*, 2022). The carbonyl group in amino acid residues and proteins confers a robust binding capacity to metals, suggesting that proteins could form a layer around metal NPs, thus preventing their aggregation and stabilizing them in the medium (Huang *et al.*, 2007).

The XRD pattern of the synthesized nanoparticles revealed four distinct peaks at angles of 111, 200, 220, and 311, which is consistent with the findings of other researchers (Mittal *et al.*, 2013; Allafchian *et al.*, 2018; Saratale *et al.*, 2020). This pattern shows sharp peaks, indicating the remarkable crystalline nature of silver nanoparticles and the presence of organic compounds such as flavonoids and phenols, which are responsible for both the reduction and stabilization of silver ions in the biosynthesized silver nanoparticles (Roopan *et al.*, 2013). The presence of multiple diffraction peaks suggested the size of the crystals in nano dimensions.

These findings were consistent with the previous ones (Firdhouse *et al.*, 2012; Kumar *et al.*, 2010; Sivakumar *et al.*, 2011), that highlighted the potential of thistle and purslane seed extracts as a promising source for the production of AgNPs. Similar results have been reported for the production of AgNPs in sizes from 2 to 75 nm using plant extracts as reducing agents (Chandran *et al.*, 2006; Tripathy *et al.*, 2010; Salari *et al.*, 2019). Synthesized silver nanoparticles using the extract of *Berberis vulgaris* indicated a size between 30 and 70 nm (Behravan *et al.*, 2019).

In Gram-positive bacteria, the cell is enclosed by a thick peptidoglycan layer made of linear polysaccharide chains with peptide cross-linking, which results in a firmer structure and increased difficulty for the penetration of silver nanoparticles. Conversely, Gram-negative bacterial cells have a thinner peptidoglycan layer (Shrivastava *et al.*, 2007). However, the effectiveness of nanoparticles against bacteria is influenced by the variation in the bacterial cell wall. Published reports on the antibacterial activity of AgNPs against Gram-negative and Gram-positive bacteria indicate that AgNPs show more antibacterial activity against Gram-negative bacteria, while they show limited activity against Gram-positive bacteria (Khandel *et al.*, 2018; Durgawale *et al.*, 2019). Despite the presentation of various theories to explain the antibacterial effects of silver nanoparticles, how AgNPs work against bacteria is not yet fully understood. Some of these theories include the generation of reactive oxygen species (ROS), the release of Ag+ ions from AgNPs binding with sulfhydryl groups to denature proteins, and the attachment of AgNPs onto bacteria leading to subsequent damage (Durgawale *et al.*, 2019).

The current antibacterial and antifungal assay suggests that AgNPs have significant effects in fighting bacteria and fungi. These effects are believed to be due to the perforation of microbial cell membranes or the generation of ROS by nanoparticles (Li *et al.*, 2008). Nanoparticles can effectively penetrate cell membranes through tiny pores, leading to mineral imbalance and leakage of intracellular proteins and enzymes, ultimately causing cell growth suppression and death. Moreover, silver has been shown to have more potent antimicrobial activity compared to copper, mercury, tin, chromium, and lead (Chen *et al.*, 2005). The use of *Artocarpus heterophyllus* L. seed extract as a reducing agent for producing nanoparticles and testing the resulting nanoparticles on Gram-positive and Gram-negative bacteria showed a very good inhibitory effect on the growth and proliferation of both groups of bacteria (Jagtap *et al.*, 2013). Furthermore,

Abdel-Aziz *et al.* (2014) reported the synthesis of silver particles using *Chenopodium murale* leaf extract and showed that the nanoparticles prepared by this method possessed strong antimicrobial and antioxidant properties. Additionally, the investigation of the antibacterial properties of nanoparticles obtained from *Azadirachta indica* leaf extract revealed that the created nanoparticles exhibited antibacterial effects on both Gram-positive and Gram-negative bacteria (Harjai *et al.*, 2013). These findings are in line with the results of the current research. The observed antibacterial and antifungal properties of AgNPs have sparked considerable interest in their potential applications. These studies have demonstrated the effectiveness of AgNPs in disrupting microbial cell membranes and inducing the generation of ROS, which leads to the suppression of cell growth and death. These collective findings emphasize the potential of nanoparticle-based interventions in combating microbial infections and highlight the importance of further exploration in this area.

CONCLUSION

In conclusion, as a readily available plant source, *S. marianum* and *P. oleracea* seed extract effectively acted as a reducing and capping agent for the production of highly stable AgNPs. X-ray diffraction pattern for structural analysis indicated high purity of biosynthesized AgNPs. In addition, AgNPs synthesized with aqueous extracts of *S. marianum* and *P. oleracea* have significant antibacterial and antifungal activity against several multi-drug resistant human pathogens such as *S. aureus*, *E. coli*, as well fungi of *F. graminearum*, and *A. alternata*. As a result, as an available plant source, the aqueous extract of these plants can effectively act as a reductant and coating agent for the production of highly stable silver nanoparticles. The use of these plant extracts can offer a sustainable and eco-friendly alternative to traditional chemical methods for synthesizing silver nanoparticles. Additionally, the natural compounds present in the plant extract can provide additional benefits such as antimicrobial and antioxidant properties, making them a versatile and valuable resource for various applications in nanotechnology and biomedicine.

ACKNOWLEDGEMENTS

Conflicts of interest
The authors declare that they have no conflict of interest.

REFERENCES

Abdel-Aziz M. S., Shaheen M. S., El-Nekeety A. A., and Abdel-Wahhab M. A. (2014). Antioxidant and antibacterial activity of silver nanoparticles biosynthesized using *Chenopodium murale* leaf extract. *Journal of Saudi Chemical Society*, 18(4): 356-363.

Afify T., Saleh H., and Ali Z. (2017). Structural and morphological study of gamma-irradiation synthesized silver nanoparticles. *Polymer Composites,* 38: 2687-2694.

Ahmad N., Sharma S., Alam M. K., Singh V., Shamsi S., Mehta B., and Fatma A. (2010). Rapid synthesis of silver nanoparticles using dried medicinal plant of basil. *Colloids and Surfaces B: Biointerfaces,* 81: 81-86.

Ahmed M., Fatima H., Qasim M., and Gul B. (2017). Polarity directed optimization of phytochemical and *in vitro* biological potential of an indigenous folklore: Quercus dilatata Lindl. ex Royle. *BMC Complementary and Alternative Medicine,* 17: 1-16.

Ajitha B., Reddy Y. A. K., and Reddy P. S. (2015). Green synthesis and characterization of silver nanoparticles using *Lantana camara* leaf extract. *Materials Science and Engineering,* 49: 373-381.

Allafchian A. R., Jalali S. A. H., Aghaei F., and Farhang H. R. (2018). Green synthesis of silver nanoparticles using *Glaucium corniculatum* (L.) curtis extract and evaluation of its antibacterial activity. *IET Nanobiotechnology,* 12: 574-578.

Al-Enazi N. M., Alsamhary K., Ameen F., and Kha M. (2023). Plant extract-mediated synthesis cobalt doping in zinc oxide nanoparticles and their *in vitro* cytotoxicity and antibacterial performance. *Heliyon*, 9(9): e19659.

Asghari G., Varshosaz J., and Shahbazi N. (2014). Synthesis of silver nanoparticle using *Portulaca oleracea* L. extracts. *Nanomedicine Journal,* 1: 94-99.

Barkai-Golan R., and Paster N. (2008). Mouldy fruits and vegetables as a source of mycotoxins: part 1. *World Mycotoxin Journal,* 1: 147-159.

Basavaraja S., Balaji S. D., Lagashetty A., Rajasab A. H., and Venkataraman A. (2008). Extracellular biosynthesis of silver nanoparticles using the fungus *Fusarium semitectum*. *Materials Research Bulletin,* 43: 1164-1170.

Behravan M., Panahi A. H., Naghizadeh A., Ziaee M., Mahdavi R., and Mirzapour A. (2019). Facile green synthesis of silver nanoparticles using *Berberis vulgaris* leaf and root aqueous extract and its antibacterial activity. *International Journal of Biological Macromolecules,* 124: 148-154.

Bhuyar P., Rahim M. H. A., Sundararaju S., Ramaraj R., Maniam G. P., and Govindan N. (2020). Synthesis of silver nanoparticles using marine macroalgae *Padina* sp. and its antibacterial activity towards pathogenic bacteria. *Beni-Suef University Journal of Basic and Applied Sciences,* 9: 1-15.

Brown N. A., Urban M., Van de Meene A. M., and Hammond-Kosack K. E. (2010). The infection biology of *Fusarium graminearum*: defining the pathways of spikelet to spikelet colonisation in wheat ears. *Fungal Biology,* 114: 555-571.

Chandran S. P., Chaudhary M., Pasricha R., Ahmad A., and Sastry M. (2006). Synthesis of gold nanotriangles and silver nanoparticles using *Aloevera* plant extract. *Biotechnology Progress,* 22: 577-583.

Chen S., Webster S., Czerw R., Xu J., and Carroll D. L. (2004). Morphology effects on the optical properties of silver nanoparticles. *Journal of Nanoscience and Nanotechnology,* 4: 254-259.

Chen S., Wu G., and Zeng H. (2005). Preparation of high antimicrobial activity thiourea chitosan–Ag+ complex. *Carbohydrate Polymers,* 60: 33-38.

Cullity B. D. (1956). *Elements of X-ray Diffraction.* Addison-Wesley Publishing.

Devanesan S., and AlSalhi M. S. (2021). Green synthesis of silver nanoparticles using the flower extract of *Abelmoschus esculentus* for cytotoxicity and antimicrobial studies. *International Journal of Nanomedicine*, 16: 3343-3356.

Dorman H. D., and Deans S. G. (2000). Antimicrobial agents from plants: antibacterial activity of plant volatile oils. *Journal of Applied Microbiology*, 88: 308-316.

Dousti B., Nabipour F., and Hajiamraei A. (2019a). Green synthesis of silver nanoparticle by using the aqueous extract of *Fumaria Parviflora* and investigation of their antibacterial and antioxidant activities. *Razi Journal of Medical Sciences,* 26: 105-117.

Dousti B., Nabipour F., and Hajiamraei A. (2019b). Green synthesis of silver nanoparticle using aqueous extract of *Fumaria Parviflora* and study of its antibacterial and antioxidant properties. *Razi Journal of Medical Sciences,* 26: 105-117.

Duan S., Guan X., Lin R., Liu X., Yan Y., et al. (2015). Silibinin inhibits acetylcholinesterase activity and amyloid β peptide aggregation: A dual-target drug for the treatment of Alzheimer's disease. *Neurobiology of Aging,* 36: 1792-1807.

Durgawale T. P., Khanwelkar C. C., and Durgawale P. P. (2019). Biosynthesis of silver nanoparticles using extracts of two species of *Portulaca* and their antibacterial activity. *International Journal of Pharmaceutical Sciences and Research,* 10: 2250-2256.

Elemike E. E., Onwudiwe D. C., Ekennia A. C., and Jordaan A. (2018). Synthesis and characterisation of silver nanoparticles using leaf extract of *Artemisia afra* and their *in vitro* antimicrobial and antioxidant activities. *IET Nanobiotechnology,* 12: 722-726.

Fahes A., Naciri A. E., Shoker M. B., and Akil S. (2023). Self-assembly-based integration of Ag-Au oligomers and core/shell nanoparticles on polymer chips for efficient sensing devices. *Soft Matter*, 19(2): 321-330.

Farshbaf M., Valizadeh H., Panahi Y., Fatahi Y., Chen M., Zarebkohan A., and Gao H. (2022). The impact of protein corona on the biological behavior of targeting nanomedicines. *International Journal of Pharmaceutics*, 614: 121458.

Fatima H., Khan K., Zia M., Ur-Rehman T., Mirza B., and Haq I.-u. (2015). Extraction optimization of medicinally important metabolites from *Datura innoxia* Mill.: an in vitro biological and phytochemical investigation. *BMC Complementary and Alternative Medicine,* 15: 1-18.

Firdhouse M. J., and Lalitha P. (2012). Green synthesis of silver nanoparticles using the aqueous extract of *Portulaca oleracea* (L.). *Asian Journal of Pharmaceutical and Clinical Research,* 6: 92-94.

Flieger J., Franus W., Panek R., Szymańska-Chargot M., Flieger W., Flieger M., and Kołodziej P. (2021). Green synthesis of silver nanoparticles using natural extracts with proven antioxidant activity. *Molecules*, 26(16): 4986.

Fouda A., Abdel-Nasser M., Eid A. M., Hassan S. E. D., et al. (2023). An Eco-friendly approach utilizing green synthesized titanium dioxide nanoparticles for leather conservation against a fungal strain, *Penicillium expansum* AL1, involved in the biodeterioration of a historical manuscript. *Biology*, 12(7): 1025.

Gupta O., Sing S., Bani S., Sharma N., Malhotra S., Gupta B., Banerjee S., and Handa S. (2000). Anti-inflammatory and anti-arthritic activities of silymarin acting through inhibition of 5-lipoxygenase. *Phytomedicine,* 7: 21-24.

Harjai K., Bala A., Gupta R. K., and Sharma R. (2013). Leaf extract of *Azadirachta indica* (neem): a potential antibiofilm agent for *Pseudomonas aeruginosa*. *Pathogens and Disease*, 69(1): 62-65.

Huang H., and Yang X. (2004). Synthesis of polysaccharide-stabilized gold and silver nanoparticles: a green method. *Carbohydrate Research,* 339: 2627-2631.

Huang J., Li Q., Sun D., Lu Y., Su Y., et al. (2007). Biosynthesis of silver and gold nanoparticles by novel sundried *Cinnamomum camphora* leaf. *Nanotechnology,* 18: 105104.

Iranshahy M., Javadi B., Iranshahi M., Jahanbakhsh S. P., Mahyari S., Hassani F. V., and Karimi G. (2017). A review of traditional uses, phytochemistry and pharmacology of *Portulaca oleracea* L. *Journal of Ethnopharmacology,* 205: 158-172.

Jacob S. J. P., Finub J., and Narayanan A. (2012). Synthesis of silver nanoparticles using *Piper longum* leaf extracts and its cytotoxic activity against Hep-2 cell line. *Colloids and Surfaces B: Biointerfaces,* 91: 212-214.

Jagtap U. B., and Bapat V. A. (2013). Green synthesis of silver nanoparticles using *Artocarpus heterophyllus* Lam. seed extract and its antibacterial activity. *Industrial Crops and Products*, 46: 132-137.

Jha A. K., Prasad K., Prasad K., and Kulkarni A. (2009). Plant system: nature's nanofactory. *Colloids and*

Surfaces B: Biointerfaces, 73: 219-223.

Kalaiarasi R., Prasannaraj G., and Venkatachalam P. (2013). A rapid biological synthesis of silver nanoparticles using leaf broth of *Rauvolfia tetraphylla* and their promising antibacterial activity. *Indo American Journal of Pharmaceutical Research,* 3: 8052-8062.

Kaviya S., Santhanalakshmi J., Viswanathan B., Muthumary J., and Srinivasan K. (2011). Biosynthesis of silver nanoparticles using *Citrus sinensis* peel extract and its antibacterial activity. *Spectrochimica Acta Part A: Molecular and Biomolecular Spectroscopy,* 79: 594-598.

Khandel P., Shahi S. K., Soni D. K., Yadaw R. K., and Kanwar L. (2018). *Alpinia calcarata*: potential source for the fabrication of bioactive silver nanoparticles. *Nano Convergence,* 5: 1-17.

Kim S. W., Jung J. H., Lamsal K., Kim Y. S., Min J. S., and Lee Y. S. (2012). Antifungal effects of silver nanoparticles (AgNPs) against various plant pathogenic fungi. *Mycobiology,* 40: 53-58.

Kumar V., Yadav S. C., and Yadav S. K. (2010). Syzygium cumini leaf and seed extract mediated biosynthesis of silver nanoparticles and their characterization. *Journal of Chemical Technology & Biotechnology,* 85: 1301-1309.

Li Q., Mahendra S., Lyon D. Y., Brunet L., Liga M. V., Li D., and Alvarez P. J. (2008). Antimicrobial nanomaterials for water disinfection and microbial control: potential applications and implications. *Water Research,* 42: 4591-4602.

Liperoti R., Vetrano D. L., Bernabei R., and Onder G. (2017). Herbal medications in cardiovascular medicine. *Journal of the American College of Cardiology,* 69: 1188-1199.

Maiti S., Krishnan D., Barman G., Ghosh S. K., and Laha J. K. (2014). Antimicrobial activities of silver nanoparticles synthesized from *Lycopersicon esculentum* extract. *Journal of Analytical Science and Technology,* 5: 1-7.

Malekinejad H., Rezabakhsh A., Rahmani F., and Hobbenaghi R. (2012). Silymarin regulates the cytochrome P450 3A2 and glutathione peroxides in the liver of streptozotocin-induced diabetic rats. *Phytomedicine,* 19: 583-590.

Mishra A., Kumari M., Pandey S., Chaudhry V., Gupta K., and Nautiyal C. (2014). Biocatalytic and antimicrobial activities of gold nanoparticles synthesized by *Trichoderma* sp. *Bioresource Technology,* 166: 235-242.

Mittal A. K., Chisti Y., and Banerjee U. C. (2013). Synthesis of metallic nanoparticles using plant extracts. *Biotechnology Advances,* 31: 346-356.

Nikbakht M., and Pour Ali P. (2015). Biological Production and antibacterial effect of synthesized Ag with aqua extract and methanol anab. *Medical Science Journal of Islamic Azad Univesity,* 12: 112-118.

Niveditha K., and Sukirtha T. (2018). Green synthesis, characterization and antimicrobial activity of silver nanoparticles from *Plectranthus amboinicus* plant extracts. *Indian Journal of Medical Research and Pharmaceutical Sciences,* 5: 2349-5340.

Okafor F., Janen A., Kukhtareva T., Edwards V., and Curley M. (2013). Green synthesis of silver nanoparticles, their characterization, application and antibacterial activity.

International Journal of Environmental Research and Public Health, 10: 5221-5238.

Poulose S., Panda T., Nair P. P., and Theodore T. (2014). Biosynthesis of silver nanoparticles. *Journal of Nanoscience and Nanotechnology,* 14(2): 2038-2049.

Pungle R., Nile S. H., Makwana N., Singh R., Singh R. P., and Kharat A. S. (2022). Green synthesis of silver nanoparticles using the *Tridax Procumbens* plant extract and screening of its antimicrobial and anticancer activities. *Oxidative Medicine and Cellular Longevity*, 2022: 9671594.

Rahimi R., Nikfar S., Larijani B., and Abdollahi M. (2005). A review on the role of antioxidants in the management of diabetes and its complications. *Biomedicine & Pharmacotherapy,* 59: 365-373.

Rajoriya P., Misra P., Singh V. K., Shukla P. K., and Ramteke P. W. (2017). Green synthesis of silver nanoparticles. *Biotech Today: An International Journal of Biological Sciences*, 7: 7-20.

Roopan S. M., Madhumitha G., Rahuman A. A., Kamaraj C., Bharathi A., and Surendra T. (2013). Low-cost and eco-friendly phyto-synthesis of silver nanoparticles using *Cocos nucifera* coir extract and its larvicidal activity. *Industrial Crops and Products,* 43: 631-635.

Sajadi S. M., Nasrollahzadeh M., and Maham M. (2016). Aqueous extract from seeds of *Silybum marianum* L. as a green material for preparation of the Cu/Fe3O4 nanoparticles: a magnetically recoverable and reusable catalyst for the reduction of nitroarenes. *Journal of Colloid and Interface Science*, 469: 93-98.

Salari S., Esmaeilzadeh Bahabadi S., Samzadeh-Kermani A., and Yosefzaei F. (2019). *In-vitro* evaluation of antioxidant and antibacterial potential of green-synthesized silver nanoparticles using *Prosopis farcta* fruit extract. *Iranian Journal of Pharmaceutical Research,* 18: 430-455.

Sivalingam A. M., Pandian A., Rengarajan S., Ramasubbu R., Parasuraman G., Sugumar V., and Devaraj N. (2023). Extraction, biosynthesis, and characterization of silver nanoparticles for its enhanced applications of antibacterial activity using the *Silybum marianum* Linn. plant. *Biomass Conversion and Biorefinery*, 1-12. DOI: https://doi.org/10.1007/s13399-023-04907-1.

Saratale G. D., Saratale R. G., Cho S.-K., Ghodake G., Bharagava R. N., Park Y., Mulla S. I., Kim D.-S., Kadam A., and Nair S. (2020). Investigation of photocatalytic degradation of reactive textile dyes by *Portulaca oleracea*-functionalized silver nanocomposites and exploration of their antibacterial and antidiabetic potentials. *Journal of Alloys and Compounds,* 833: 155083.

Schulz V., Hänsel R., and Tyler V. E. (2001). Rational phytotherapy: a physician's guide to herbal medicine. 4th Edition, Springer-Verlag, Berlin, Heidelberg. DOI: http://dx.doi.org/10.1007/978-3-642-98093-0.

Sharma G., Sharma A. R., Lee S.-S., Bhattacharya M., Nam J.-S., and Chakraborty C. (2019). Advances in nanocarriers enabled brain targeted drug delivery across blood brain barrier. *International Journal of*

Pharmaceutics, 559: 360-372.

Sharma N. C., Sahi S. V., Nath S., Parsons J. G., Gardea-Torresde J. L., and Pal T. (2007). Synthesis of plant-mediated gold nanoparticles and catalytic role of biomatrix-embedded nanomaterials. *Environmental Science & Technology,* 41: 5137-5142.

Shrivastava S., Bera T., Roy A., Singh G., Ramachandrarao P., and Dash D. (2007). Characterization of enhanced antibacterial effects of novel silver nanoparticles. *Nanotechnology,* 18: 225103.

Singh R., and Kumari N. (2020). *Sapindus mukprossi* Gaertn.: Rich source of antioxidants and reducing agents. *Ethics and the Environment,* 24: 38-46.

Singh R. P., Gu M., and Agarwal R. (2008). Silibinin inhibits colorectal cancer growth by inhibiting tumor cell proliferation and angiogenesis. *Cancer Research,* 68: 2043-2050.

Sivakumar J., Premkumar C., Santhanam P., and Saraswathi N. (2011). Biosynthesis of silver nanoparticles using *Calotropis gigantean* leaf. *African Journal of Basic & Applied Sciences (AJBAS)*, 3: 265-270.

Škottová N., and Krečman V. (1998). Silymarin as a potential hypocholesterolaemic drug. *Physiological Research*, 47: 1-7.

Tan M., Wang G., Ye Z., and Yuan J. (2006). Synthesis and characterization of titania-based monodisperse fluorescent europium nanoparticles for biolabeling. *Journal of Luminescence*, 117: 20-28.

Tripathy A., Raichur A. M., Chandrasekaran N., Prathna T., and Mukherjee A. (2010). Process variables in biomimetic synthesis of silver nanoparticles by aqueous extract of *Azadirachta indica* (Neem) leaves. *Journal of Nanoparticle Research,* 12: 237-246.

Vickers N. J. (2017). Animal communication: when i'm calling you, will you answer too? *Current Biology,* 27: R713-R715.

Vijayaraghavan K., Nalini S. K., Prakash N. U., and Madhankumar D. (2012). Biomimetic synthesis of silver nanoparticles by aqueous extract of *Syzygium aromaticum*. *Materials Letters,* 75: 33-35.

Wang P., and Aguirre A. (2018). New strategies and in vivo monitoring methods for stem cell-based anticancer therapies. *Stem Cells International,* 2018: 7315218.